Gap-related magnetic characteristics of magnetorheological dampers with porous metal foam

XING-YAN YAO[a,*], ZHIZHAO PENG[b]
[a]*Chongqing Engineering Laboratory for Detection Control and Integrated System, Chongqing Technology and Business University, Chongqing 400067, China*
[b]*Army Academy of Armored Forces, Fengtai, Beijing 100072, China*

Magnetorheological (MR) dampers are used to reduce and control vibrations. An approach that includes porous metal foam to store the magnetorheological fluid has been proposed to increase the lifespan of MR dampers and save cost. However, the magnetic field in the shear gap is a key factor which determines the damper's performance. And the magnetic characters inside the shear gap is difficult to measurement by experiments. This paper investigates the magnetic characteristics of porous metal foam MR dampers using magneto-static model in Ansys, and the field distribution inside the shear gap was obtained. The simulation results show that the magnetic flux density in the shear gap increases by adding porous metal foam to the inner wall of the cylinder. The magnetic flux density increases with current increment while decreases as the gap distance increased.

(Received February 19, 2018; accepted November 29, 2018)

Keywords: Magnetorheological (MR) dampers, MR fluid, Porous metal foam, Magnetic characteristic

1. Introduction

Magnetorheological (MR) fluid is a smart material that can transition from a Newtonian fluid to a non-Newtonian fluid in a few milliseconds by applying an external magnetic field. This transition is reversible and is known as MR effect [1, 2]. MR fluid is composed of micro-magnetic particles, continuum fluid and additives. Typically, petroleum based oils, silicone, mineral oils, water and others are used as continuum fluid. The additives are used to provide additional lubricating properties to inhibit sedimentation and agglomeration.

MR fluid has been widely used in areas of vibration control, vehicle suspension, et al. In particular, MR dampers are popular due to their controlled damping force and fast response time. Many studies [4-7] have focused on the large damping force provided by MR dampers in civil applications, vehicle suspension systems, and medical devices. Lord Corporation has developed a minimum damper series, RD1097, however, the damping force is still almost 100 N [8]. Due to the emergence of micro-systems and micro-machines, demanding for low damping force has been increasing [9-12]. For instance, a stable load of 5 N is reasonable for the bounding pressure of microelectronics packaging equipment, while the damping force is only 20 N for micromechanical systems.

Li [13, 14] proposed a small-MR fluids damper with an outer electromagnetic coil and silicon steel. When the coil current ranged from 0 A to 0.8 A, the damping force changed from 18 N to 55 N. Tse [15] introduced a small-scale shear-mode rotary MR damper for wind tunnel testing, and the maximum shear damping force is 4 N.

All of the above-mentioned MR dampers in the cylinder must be filled with MR fluids, and require a precision sealing structure to prevent leakage of the MR fluids. Moreover, the moving piston rod leads to surface abrasion to accelerate the leakage. Because of the resulting high cost and short lifetime resulting from these issues, the MR damper has not been widely implemented.

Carlson [16] proposed a novel MR fluid damper which uses a porous sponge wrapped around the piston to reduce the damper cost. In this case, the MR fluids are saturated in a layer of open-celled, polyurethane foam without any seals or bearings, and only 3 ml of MR fluids is used. The maximum damping force is 150N when the excited current is 2A. This type of MR fluid sponge damper can be used to control vibration with moderate force. Although the use of porous sponge can solve the problems of sealing, service life and cost of MR damper to a certain extent, the porous sponge is easy to wear and the hardness is low, which short the life time of the damper. Furthermore, in the process of piston movement, the shear gap will change due to the thickness of the sponge changes, the output damping force is not easy to control. Hence, Yao et al. [17] proposed a new porous metal foam MR damper. The MR fluid is stored in porous metal foam when the magnetic field is zero; as soon as the external magnetic field exceeds a critical value, the MR fluid is expelled from the porous metal foam into the shear gap to produce the damping force. Compared with traditional MR dampers, this structural design can reduce the cost of MR damper by using the porous metal foam to store and release the MR fluids without any sealing. The lifetime of porous metal foam MR dampers is longer because porous metal foam is stronger the porous sponge. Metal foam MR fluid materials can also be used without sealing and provide a long service life.

Previous studies [17-23] show that the normal force of MR fluids filled with porous metal foam and the dynamic response time of porous metal foam MR dampers are

different than those of traditional MR dampers. Because the porous metal foam is added in the cylinder, there is a significant difference for the porous metal foam MR damper. Under the influence of external currents, MR fluids should be firstly extracted from porous metal foam to the shear gap, and then move with the piston. The magnetic properties play a significant role of the performance and applications of MR dampers, especially the porous metal foam ones.

The magnetic field in the shear gap is a crucial factor that determines how the performance of the damper, and this is very difficult to determine from experimentation. In this paper, after introducing the magnetic path of the proposed MR damper, the magnetic resistance of porous metal foam filled with MR fluids is demonstrated by calculating and finite element analysis of Ansys. The effects of metal foam Cu, shear gap width, external currents on the magnetic flux density are investigated. The magnetic flux density in shear gaps with effect of porous metal foam Cu also demonstrated.

2. Porous metal foam MR dampers

Fig. 1 is a schematic of the porous metal foam damper prototype studied in this article. The porous foam material is adhered to the inside of the working cylinder before injecting MR fluids. The magnetic field path is composed of the cylinder, porous metal foam, shear gap, and piston. Both ends of the cylinder have a 2-mm piece of bronze to make sure the magnetic flux flows along the expected route. Generally, porous metal foams are made from an open-cell metal material with a preferred porosity of 80% or more. When the external current is zero, the MR fluids are stored in the porous metal foam. When the current is large enough, the MR fluids are drawn out from the porous metal foams and then begin to fill the shear gap. Therefore, the MR fluids effect is produced.

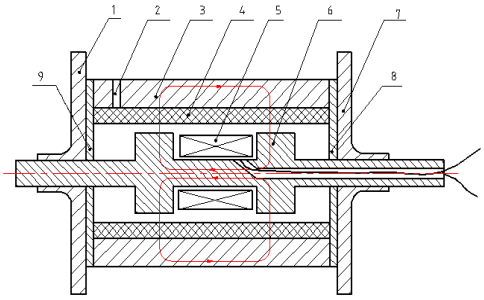

Fig. 1. Porous metal foam MR damper: 1,7 End cap of cylinder Piston rod; 2 Gap; 3 Cylinder; 4 Porous metal foam; 5 Coil; 6 Piston; 8,9 Bronze

3. Magnetic resistance model

Fig. 2 shows the magnetic circuits of the proposed damper. The magnetic resistance is calculated by equation (1).

$$R = R_1 + 2R_2 + R_{wall} + 2R_{gap} + 2R_{foam} + 2R_{mrf} \quad (1)$$

where μ_p is 3.54; R is 1.07 × 106 A/wb, R_1 and R_2 are the magnetic resistances of the piston; R_{wall} and R_{gap} are the magnetic resistances for the cylinder wall and shear gap, and R_{foam} is the resistance of the porous metal foam filled with MR fluid, respectively. Fig. 3 describes the equivalent magnetic resistance of the porous foam metal MR damper.

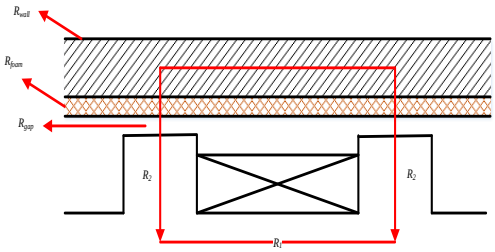

Fig. 2. Magnetic resistance calculation of porous foam metal MR damper

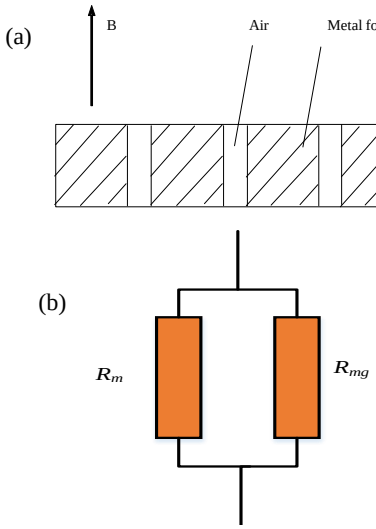

Fig. 3. Magnetic resistance models for metal foam filled with MR fluid: (a) computational model; (b) magnetic resistance model

The equivalent magnetic resistance of metal foam in Fig. 3. The magnetic resistance is depicted in equations (2) and (3).

$$\frac{1}{R_p} = \frac{1}{R_m} + \frac{1}{R_{mg}} \quad (2)$$

$$R = \frac{L}{m_0 m_r A} \quad (3)$$

Where R_p is the equivalent magnetic resistance of porous metal foam filled with MR fluid; R_m and R_{mg} are the magnetic resistance of porous metal foam and MR fluid, respectively; R is the magnetic resistance; L is length; μ_r is relative permeability; and μ_0 is vacuum permeability.

Finally, the relative permeability of porous metal foam filled with MR fluids is

$$m_p = m_m S_m + m_{mg} S_{mg} \quad (4)$$

where S_m is the proportion of metal and S_{mg} is the porosity of the porous metal foam and μ_m and μ_p are relative permeability of foam meatal and relative permeability of foam meatal full of MR fluid, respectively.

4. Simulation of magnetic characteristic

4.1. Materials used in simulation

The specimen is MR Fluid-J01T from Chongqing Instrument Materials Institute, the shear viscosity at 20 ℃ is 0.8 Pa.s when the magnetic field is zero, and the average diameter of the MR particles is around 1–5 μm. Fig. 4. depicts the magnetic characteristics. The density (g/cm^3) is ρ. PPI is the pore size. The properties of the porous metal foam Cu used in this study are depicted in Table 1. Table 2 gives the calculation result of the magnetic induction intensity of porous metal foam Cu, from which we can obtain that B = 0.591I.

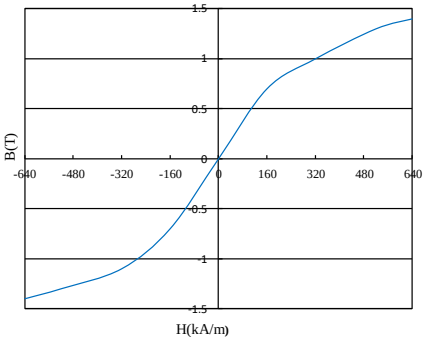

Fig. 4. Magnetic characteristics of MR fluid

Table 1. Properties of porous metal foam Cu

Metal foam	μ	ρ	PPI	Porosity (%)	Thickness (mm)
Cu	1	0.26	110	85	2

Table 2. Magnetic induction intensity of porous metal foam Cu

Material	μ	R(A/wb)	B（T）
Cu	1	1.159×10^6	0.591I

4.2. Results and discussion

Fig. 5 and Fig. 6 gives the distribution of the magnetic flux line and the contour of the magnetic flux density, respectively. Here, the thickness of the porous metal foam Cu is 2 mm, the shear gap is 1 mm, and the external current is 2 A. Fig. 5 and Fig. 6 show that most of magnetic flux lines go through the shear gap. The leakage of magnetic flux density can be neglected.

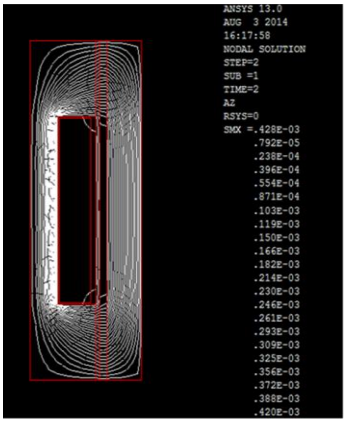

Fig. 5. Distribution of magnetic flux line

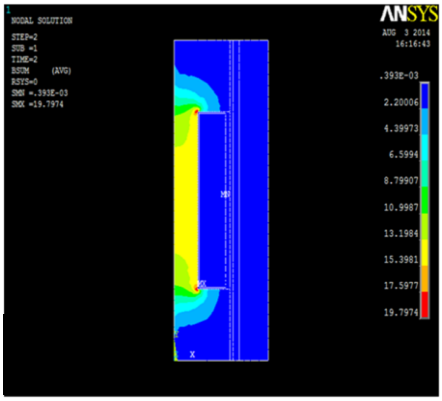

Fig. 6. Contour of magnetic flux density

Fig. 7 shows the magnetic flux density in the shear gap with the effect of porous metal foam. Five currents (0 A, 0.5 A, 1 A, 1.5 A, 2 A) were used. The blue columns describe the magnetic flux density in the shear gap without any porous metal foam. The magnetic flux density when the porous metal foam Cu is pasted to the inner wall of the cylinder are also described in the orange columns at different currents in Fig. 7. The results show that the magnetic flux density in the shear gap increases by current increment. Thus, the magnetic field intensity of the porous metal foam damper can be controlled by adjusting the current. The magnetic flux density continues to increase until the current is 1.5 A. However, even if the current keeps increasing from 1.5 A to 2 A, the magnetic flux density falls to a high equilibrium value due to the saturation of MR fluid. Moreover, the quickest increase occurs when the current ranges from 0 A to 0.5 A. When applying the current, the magnetic particles become a serial chain along the direction of the magnetic flux line in the shear gap. The larger the current, the more chains (even forming a sheet composed of magnetic particles) and magnetic flux lines. Therefore, the magnetic flux density also increases. The contour of the magnetic flux density in the shear gap is displayed in Fig. 6.

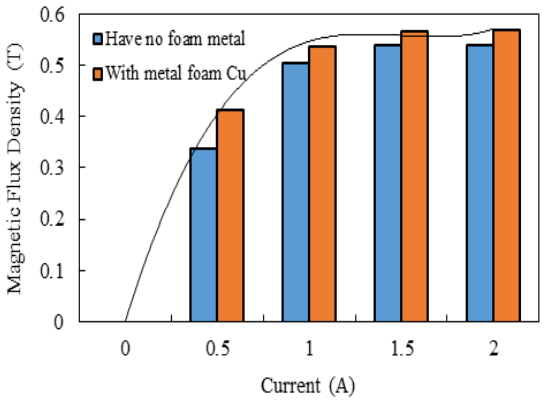

Fig. 7. Magnetic flux density in shear gap with the effect of porous metal foam

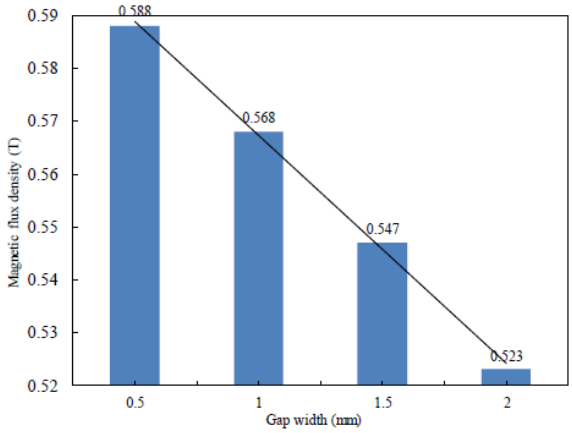

Fig. 8. Influence of currents on magnetic field in shear gap with porous metal foam Cu

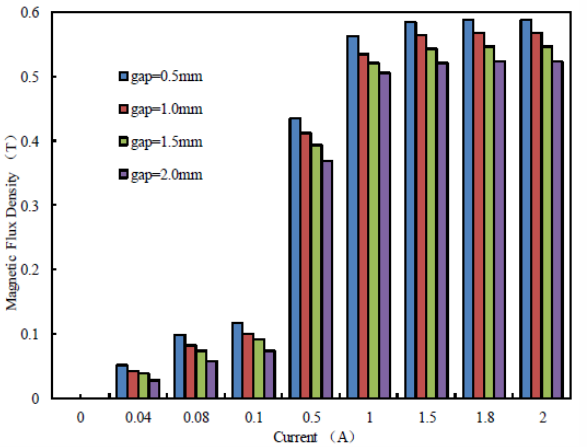

Fig. 9. Influence of shear gap on magnetic field with porous metal foam Cu

Furthermore, the magnetic flux density with porous metal foam Cu is higher than that of without any metal foam materials in the shear gap. Different porous metal foam materials lead to varying magnetic flux density in the shear gap. Since the magnetic permeability of porous metal foam Cu is 1, which is the same as the air, the difference between the magnetic flux density represented by the blue columns and the orange columns is not obvious.

In order to investigate the effect of current on magnetic flux density in different shear gaps, four different shear gaps (0.5 mm, 1 mm, 1.5 mm, and 2 mm) were used in the simulation as shown in Fig. 8. The magnetic flux density decreases lineally as the shear gap width increases. In general, the smaller the shear gap, the larger the magnetic flux density. However, the shear gap should not be too small due to the difficulty of processing. The smaller the shear gap, the higher precision of processing. Too high precision is usually difficult to obtain. Meanwhile, a shear gap that is too large will lead to a lower the magnetic flux density, which does not satisfy the application requirements. Therefore, the shear gap of the MR damper should be appropriate to the specific application. Fig. 9 gives the relationship between the current and the magnetic flux density with different shear gaps. The magnetic flux density decreases by increasing the shear gap at the same external current and increases by increasing the external currents.

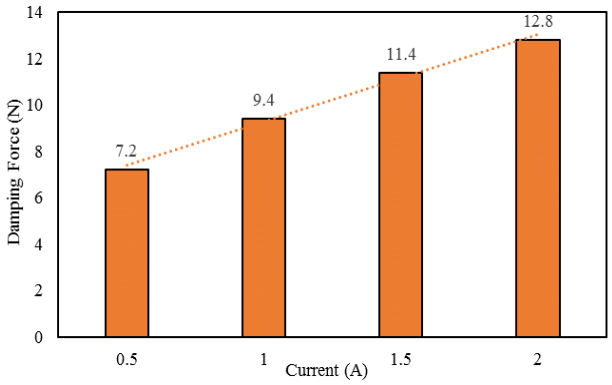

Fig. 10. Effect of porous metal foams and currents on damper force (shear velocity 6 mm/s)

Fig. 10 shows the effect of the porous metal foams on the damping force under different currents when the shear velocity is 6 mm/s. The dashed line depicts the tendency of the damping force to change with the external currents. The damping forces increase by increasing the currents. When the external current changes from 0.5 A to 2 A, the damping force ranges from 7.2 N to 12.8 N.

5. Conclusion

In this paper, the magnetic field distribution in the shear gap of porous metal foam MR dampers was investigated by calculation model and verified by simulation. The relationship between the magnetic induction intensity and the external current is B = 0.591I by calculation model. The simulation results show that most of the magnetic flux lines go through the shear gap, and the magnetic flux density increases by increasing the external currents, but decreases by gap increments. The current-increased magnetic flux density results from the increasing chains of magnetic particles in MR fluids. The

magnetic flux density in the shear gap increases by adding porous metal foam Cu to the inner wall of the cylinder, and the damping force increases by increasing the external currents.

Acknowledgments

This research is partially supported by the National Natural Science Foundation of China under grant number (No. 51605061, No. 51605490), Chongqing Research Program of Basic Research and Frontier Technology (No. cstc2017jcyjAX0183), the Science and Technology Research Project of Chongqing Municipal Education Committee (No. KJ1500627), the school projects of Chongqing Technology and Business University (No. 1552003), the startup project of Doctor scientific research (No. 2016-56-04), the Open Grant of Chongqing Engineering Laboratory for Detection Control and Integrated System.

References

[1] J. De Vicent, D. J. Klingenberg, R. Hidalgo-Alvarez, Soft Matter. **7**(8), 3701 (2011).
[2] X. Y. Yao, M. Yu, J. Fu, Smart Materials and Structures **24**(3), 035001 (2015).
[3] X. Zhu, X. Jing, L. Cheng, Journal of Intelligent Material Systems and Structures **23**(8), 839 (2012).
[4] J. M. Guldbakke, J. Hesselbach, Journal of Physics: Condensed Materials 18 (2006).
[5] G. Yang, B. F. Spencer Jr, H. J. Jung, J. D. Carlson, Journal of Engineering Mechanics **130**(9), 1107 (2004).
[6] D. H. Wang, W. H. Liao, Smart Materials and Structures **20**(2), 023001 (2011).
[7] F. Gao, Y. N. Liu, W. H. Liao, Sensors and Smart Structures Technologies for Civil, Mechanical, and Aerospace Systems **10168**, (2017).
[8] M. G. Yang, C. Y. Li, Z. Q. Chen, Engineering Structures **52**, 434 (2013).
[9] L. Su, T. Shi, L. Du, X. Lu, G. Liao, Microelectronics Reliability **55**(1), 213 (2015).
[10] L. Du, T. Shi, P. Chen, L. Su, J. Shen, J. Shao, G. Liao, Microelectronic Engineering **139**, 31 (2015).
[11] J. Li, L. Liu, L. Deng, B. Ma, F. Wang, L. Han, IEEE Electron Device Letters **32**(10), 1433 (2011).
[12] X. Lu, G. Liao, Z. Zha, Q. Xia, T. Shi, NDT & E International **44**(6), 484 (2011).
[13] J. Li, D. Wang, J. A. Duan, H. He, Y. Xia, W. Zhu, IEEE Transactions on Industrial Informatics **11**(3), 612 (2015).
[14] J. Li, W. Wang, Y. Xia, H. He, W. Zhu, Applied Physics Letters **106**(1), 014104 (2015).
[15] T. Tse, C. C. Chang, Journal of Structural Engineering **130**(6), 904 (2004).
[16] J. D. Carlson, Journal of Intelligent Material Systems and Structures **10**(8), 589 (1999).
[17] Y. X. Yao, L. X. Hui, M. Yu, J. Fu, L. H. Dong, Smart Materials and Structures **22**, 1 (2013).
[18] X. Y. Yao, C. W Liu, H. F. Qin, H. Liang, Q. Yu, C. Li, Journal of Magnetism and Magnetic Materials **403**, 161 (2016).
[19] X. Y. Yao, Z. Chen, H. Qin, Q. Yu, C. Li, Optoelectron. Adv. Mat. **10**(3-4), 253 (2016).
[20] L. X. Hui, H. Zhang, G. X. Li, X. Y. Yao, S. Meng, Optoelectron. Adv. Mat. **10**(1-2), 74 (2016).
[21] E. Du, L. Cai, K. Huang, H. Tang, X. Xu, R. Tao, Fuel 211 (2018).
[22] P. Chen, L. J. Qian, X. X. Bai, S. B. Choi, Journal of Rheology **61**(3), 455 (2017).
[23] X. X. Bai, N. M. Wereley, W. Hu, Journal of Applied Physics **117**(17), 717 (2015).

*Corresponding author: yaoxingyan-jsj@163.com